Juniper Online
Journal Material Science
ISSN: 2575-856X

Research Article
Volume 8 Issue 4 - May 2024
DOI: 10.19080/JOJMS.2024.08.555744

JOJ Material Sci

Advances in Nondestructive Evaluation and Analyses of Thermal Spray Coatings

Xinqing Ma* and Peter Ruggiero

Surface Technologies Division, Curtiss-Wright Corporation, East Windsor, USA

Submitted: May 01, 2024; **Published:** May 15, 2024

***Corresponding author:** Xinqing Ma, Surface Technologies Division, Curtiss-Wright Corporation, East Windsor, USA

Abstarct

Nondestructive Evaluation and Testing (NDE&T) techniques have been played vital roles in property characterization, process development and quality control of various thermal spray coatings. Besides conventional NDE&T lab methods such as eddy current test (ECT) for thickness measurement and fluorescent penetrant inspection (FPI) for cracking detection, some latest NDE techniques have been developed, demonstrated and applied to evaluate and characterize thermal sprayed coatings recently. The improved and innovative NDE methods provide more capable and accurate measurement to inspect on surface morphology, 2D and 3D coating porosity, oxide content, interface debonding, as well as other types of coating features, defects or specific properties. In this work, some non-contact NDE techniques and their applications were investigated and discussed based on several case studies of thermal sprayed coatings. Laser confocal microscopy had been used for characterizing surface morphologies and roughness profiles of HVOF WC-based coatings with 2D and 3D mapping methods. In particular, thermal wave imaging and ultrasonic micro imaging methods were used to detect the suspicious existence of lateral coating separation within or at the MCrAlY coating-substrate interfaces. The laser dimension sensoring method exhibited the extended capability of in-situ coating thickening measurements on turbine blade and vane. The latest non-contact NDE techniques demonstrated their unique and strong capability for in-situ and ex-situ coating characterization, process and quality control and coating failure analysis.

Keywords: Coating; NDE&T; Thermal spray; Ultrasonic; Laser sensor; Thermography

Introduction

Thermal spray coatings are commonly utilized to safeguard industrial components from environmental degradation caused by wear, erosion, corrosion, oxidation, and hot corrosion. Ensuring the effectiveness of these protective coatings requires thorough quality control and inspection. Coating quality control encompasses various aspects, including surface finish, coating thickness, defects within the coating matrix, and interface contaminations or defects. However, traditional inspection tools may not be suitable, capable, efficient, rapid, convenient, or nondestructive enough to detect these sub-surface and interface defects accurately.

Nondestructive evaluation, testing, and analysis (NDE&T) techniques have played a crucial role in characterizing properties, developing processes, and ensuring the quality control of thermal spray coatings. Compared to traditional inspection methods like eddy current, electromagnetic, and liquid penetration, NDE&T techniques offer the ability to qualitatively and quantitatively disclose and characterize sub-surface and interface defects, including cracks, pores, inclusions, separation, delamination, and variations in material properties and microstructures [1-3].

In recent years, advancements in NDT techniques, particularly non-contact techniques, have expanded their capabilities and applications in the field of surface coatings. Laser confocal imaging techniques have been employed to evaluate surface morphologies and roughness through 2D or 3D surface mapping methods [4-8]. Thermal/infrared imaging technologies, based on the principles of thermal radiation, have become increasingly popular and convenient, especially with the availability of high-resolution infrared cameras and high-performance computers [9-12]. Ultrasonic scanning imaging technologies can also be utilized to inspect internal defects within the coating by employing different scanning modes for reflective or transmitted inspection.

The focus of this study was on exploring and utilizing advanced non-contact NDE techniques to examine thermal sprayed coatings. Specifically, thermal wave imaging and ultrasonic micro imaging methods were employed to identify any potential

lateral separation in the specimens. Through these cutting-edge NDE techniques, the study showcased their exceptional ability to accurately characterize coatings, monitor the manufacturing process, ensure quality control, and conduct failure analysis.

Experimental Methods

Specimens

The preparation of coating specimens on flat substrates involved the use of the high velocity oxygen fuel (HVOF) process. The Jetkote HVOF spray system was utilized to apply coatings with a thickness ranging from 150 μm to 3 mm. Typical HVOF parameters include standoff distance 200-250 mm, powder feed rate 45-60 gram/min, working gases O_2 and H_2, with a deposition rate of 50-75 μm/pass. These coatings consisted of various materials, including metallic alloys (Ni5Al, MCrAlY), cermet composites (WC-Co or CoCr), and ceramics (ZrO_2-$8Y_2O_3$). Prior to applying the coatings, the substrate surfaces were roughened by sand blasting of #60 Al_2O_3 grits to achieve a surface average roughness Ra in the range of 2 to 3 microns. The substrate material is Inconel 718 typically. In order to analyze the surface morphology, as-sprayed specimens with unfinished surfaces were subjected to non-destructive testing (NDT). However, for certain NDT tests such as ultrasonic imaging, specimens with finely finished surfaces after grinding were predominantly used. Additionally, curved ring segment parts were coated with thick MCrAlY coatings and primarily examined at the interface between the coating and the Ni-based alloy substrate to assess coating adhesion.

Laser scanning confocal microscopy

The sample surface areas of interest were scanned using a point source laser beam in a raster pattern. Galvanometric mirrors were utilized to capture intensity values in the X, Y, and Z dimensions. The VR-3200 model of laser confocal microscopy with a motorized X-Y stage, manufactured by Keyence Corporation, was employed for this purpose. This setup allowed for instant one-shot 3D measurements over a relatively large surface area, with field-of-view dimensions of 184 mm × 88 mm in the X-Y direction. Subsequently, surface topographic images were obtained, and surface roughness was calculated based on 2D linear thickness profiles in specific areas, as well as 3D thickness maps of the entire scanned region or selected areas.

Thermograph imaging method

Infrared pulse thermography was employed as a non-destructive testing tool to identify damages or defects in the thermal sprayed samples. The infrared imaging system utilized was produced by Thermal Wave Imaging, Inc. under the model name EchoThermo®. This fully integrated system includes hardware components such as a sample stage, IR lamp, thermal camera, and others, along with software for signal processing that allows for the creation of thermal images of the coating specimens. During the testing process, the specimens were positioned on an insulating slab with the coating surface facing the IR lamp. Thermal images were captured using a flash lamp with a spot size of approximately 300 mm × 230 mm, with each flash shot lasting 5 seconds. Analysis of the temperature versus time responses enabled the derivation of information regarding the depth and sizes of defective features, coating thickness, and thermal properties from the measurements.

Ultrasonic micro imaging method

The ultrasonic or acoustic micro imaging technique was employed to examine the internal structure of the coating specimens in order to identify and assess any defects and changes in properties using high frequency ultrasonic energy. During the tests, the samples were placed in a water container with the coating surfaces positioned near the ultrasonic transducer integrated into the ultrasonic scanning system (D9600 or Gen6, Sonoscan, Inc). The objective of this examination was to assess the quality of bonding at the coating/substrate interface without the need for destructive sample cutting. C-mode scanning, a form of pulse-echo, was utilized for the inspection process, including the interface scan. The method of loss of back echo was applied to analyze the samples. The pixel sizes typically ranged from 20 to 200 μm, with frequencies varying from 20 to 200 MHz. While the high frequency resulted in high resolution images, it also limited the depth of penetration into the specimens. Optimal high-resolution images were achieved when the pixel sizes matched the transducer resolutions.

Laser thickness sensoring method

Real-time and in-situ coating thickness measurement was implemented while spray processing through the utilization of a non-contact laser sensor measurement technique. The CCD laser displacement sensor utilized for thickness measurement operated on the principle of triangulation, involving the sensor enclosure, emitted laser, and reflected laser light. For thickness measurement, a wide spot laser sensor (LK-H157, Keyence Corporation) was chosen, with key parameters such as reference distance of 150 mm, measurement range of ±40 mm, and spot dimensions of 120 μm × 4200 μm. Throughout the spray trials, the laser sensor was either mounted on a holding fixture or attached to the ABB robot equipped with a thermal spray gun. By employing a non-contact position sensor and programming the robot for manipulation, the laser sensor continuously captured thickness data before, during, and after spray processing. The real-time thickness data were displayed, monitored, and stored in the control unit memory and/or a PC via a data port. Thickness measurements were conducted during spraying on stationary, rotational, or index-rotated flat substrates and airfoil parts using either a point spot sensor or a wide spot sensor.

Results and Discussion

Surface inspection by laser confocal microscopy

The WC-CoCr coating test specimens, which were applied using two different HVOF processes, underwent examination through

How to cite this article: Xinqing M, Peter R. Advances in Nondestructive Evaluation and Analyses of Thermal Spray Coatings. JOJ Material Sci. 2024; 8(4): 555744. DOI: 10.19080/JOJMS.2024.08.555744

laser confocal microscopy. A series of images were captured using reflected light mode at various focal planes. Laser scanning was conducted over a 2 mm × 1.5 mm area to reconstruct both 2D and 3D images. Figure 1 displays the 2D images on the left and the 3D images on the right for the two coating surfaces. The coating

a) applied using the small-particle (-15μm) HVOF process, exhibits a visually smooth surface in comparison to the coating

b) applied using the coarse-particle (-45μm) HVOF process.

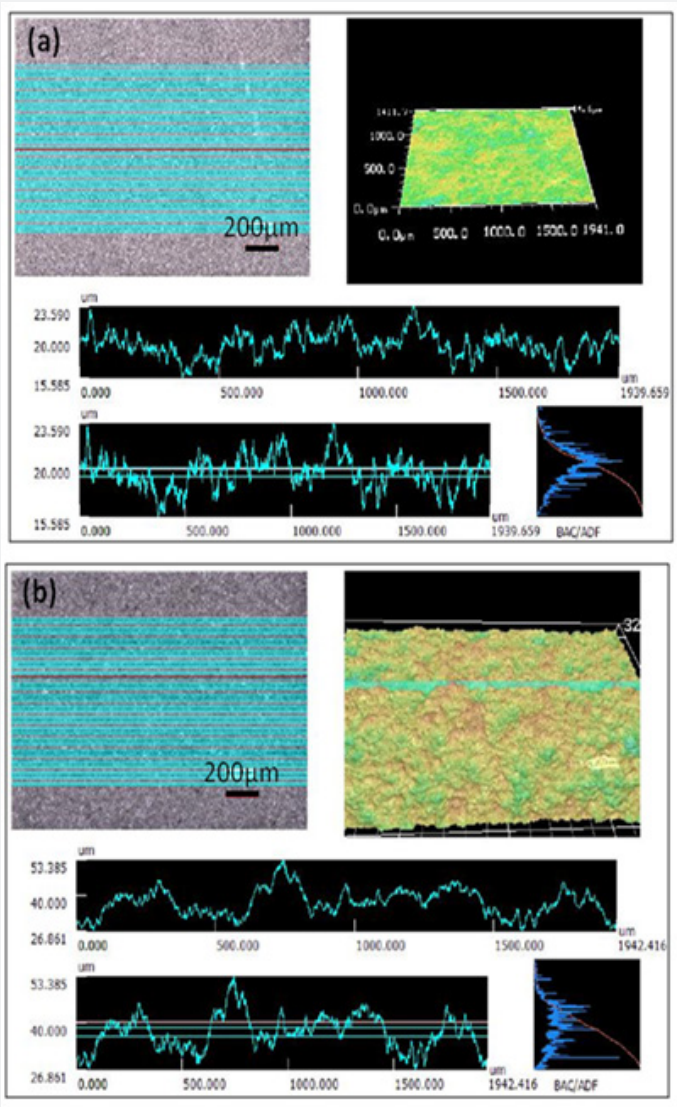

Figure 1: 2D and 3D topographic images of the coating surfaces and linear scan and mapping measurement of surface roughness of the coatings. (a) A smooth WC-CoCr coating applied by small-particle HVOF process; (b) A coarse WC-CoCr coating by large-particle HVOF process.

Surface profile data were extracted from the imaging data by scanning across a line or area of 2.0 mm × 1.0 mm on the selected surfaces as indicated in the images. Certain surface roughness parameters were computed from the surface profiles and are documented in Table 1. The parameters, such as roughness average Ra, maximum profile height Rt, standard deviation for average Ra, and maximum profile peak depth Rv, are contrasted in Table 1.

The surface roughness parameters from line-type and map-type measurements indicate that coating

a) is significantly smoother than coating

b) which was applied using large-sized feedstock.

Table 1 shows that map-type parameters offer the advantage of providing detailed information such as Ra with standard deviation and maximum Ra. Both types of measurements

How to cite this article: Xinqing M, Peter R. Advances in Nondestructive Evaluation and Analyses of Thermal Spray Coatings. JOJ Material Sci. 2024; 8(4): 555744. DOI: 10.19080/JOJMS.2024.08.555744

yield consistent results in characterizing surface roughness. In map-type measurements, the slice spacing can be adjusted for varying resolution needs. Map-type measurements offer several advantages over line-type for both coating cases. Firstly, they can provide standard deviation values (Std) for roughness measurements due to the collection of a large group of data. This allows for a more accurate assessment of the variability in roughness. Secondly, map-type measurements are capable of providing a more representative mean roughness value over a measurement area compared to a single measurement line. This is particularly beneficial for highly irregular surfaces where a single line measurement may not capture the overall roughness accurately. Additionally, map-type measurements allow for the visualization of the measured area, providing a visual image that can be used for illustration and comparison of surface morphology. Lastly, other roughness parameters such as Rt and Rv appear to be more representative and consistent when measured using map-type measurements.

Table 1: Results of surface roughness measurements using a laser confocal microscopy in line and map-modes.

Measurement	Surface Roughness Parameters, μm				
	Ra	Ra,Std.	Ra,Max.	Rt	Rv
Coating- (a)					
Line-type	1.48			10.97	5.2
Map-type	1.35	0.25	2.11	9.66	4.48
Coating- (b)					
Line-type	3.21			21.57	11.7
Map-type	3.2	0.42	4.12	20.94	9.96

Previous studies have provided more in-depth test results and analyses on the impact of spray parameters and feedstock on coating surface. This non-destructive, non-contact method is ideal for industrial control due to its speed and compatibility with traditional tactile results. Additionally, the method generates digital profiles that can be further analyzed.

Interface inspection by ultrasonic micro imaging

The turbine ring segment components were coated with MCrAlY material using HVOF spraying. Upon conducting a routine fluorescent penetrant inspection (FPI), certain coated parts exhibited questionable regions that suggested potential separation between the coating and the component. Figure 2 illustrates two defective coating areas within a coated part - one in the middle section and the other near the part's corner. The FPI examination was able to identify linear defects on the surface but lacked the ability to determine the depth of crack propagation. Consequently, ultrasonic micro imaging was employed to non-destructively detect the suspicious debonding areas within the coating sample.

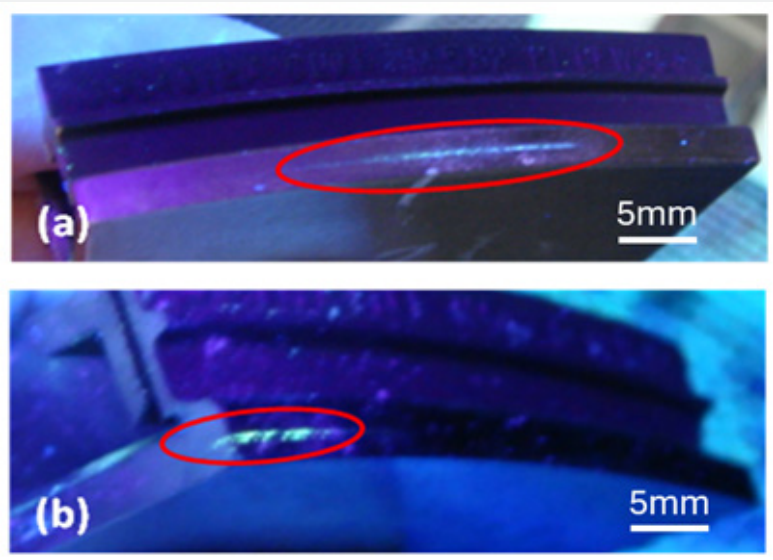

Figure 2: FPI Inspection of MCrAlY Coating applied on a Ni-based alloy part. (a) Linear defect associated with potential coating delamination at the interface is indicated in the middle section of the coating; (b) Similar linear defect is observed at a corner of the coating specimen.

How to cite this article: Xinqing M, Peter R. Advances in Nondestructive Evaluation and Analyses of Thermal Spray Coatings. JOJ Material Sci. 2024; 8(4): 555744. DOI: 10.19080/JOJMS.2024.08.555744

The ultrasonic micro imaging technique utilizes high frequency impulses and echo pulses to create a C-scan. In the presence of adhesive defects at the interface, the C-scan images will show numerous bright dots and spots against a dark background of well-adhered areas. Figure 3 displays the scan images obtained from the interface regions. Two areas highlighted as "white" indicate coating debonding/separation, which correspond to the FPI line-type defects shown in Figure 2a & 2b. The ultrasonic images provide clear information about the locations and sizes of the debonding areas. Additionally, other "white" spots may appear due to features like cooling channels in the part.

After conducting NDT inspections, the part underwent a physical cutup to verify the presence of coating delamination. Subsequently, destructive metallography was carried out using optical microscopy on suspicious sections of the cutup part. Figure 4 displays the cross-sectional microstructures of the cutup specimens. The results clearly indicate the presence of coating debonding, which initiates from the edge and extends along the coating/part interface in both pre and post-grinding operations on the side surface. The location of the coating debonding corresponds to the findings from the ultrasonic imaging inspection shown in Figure 3b.

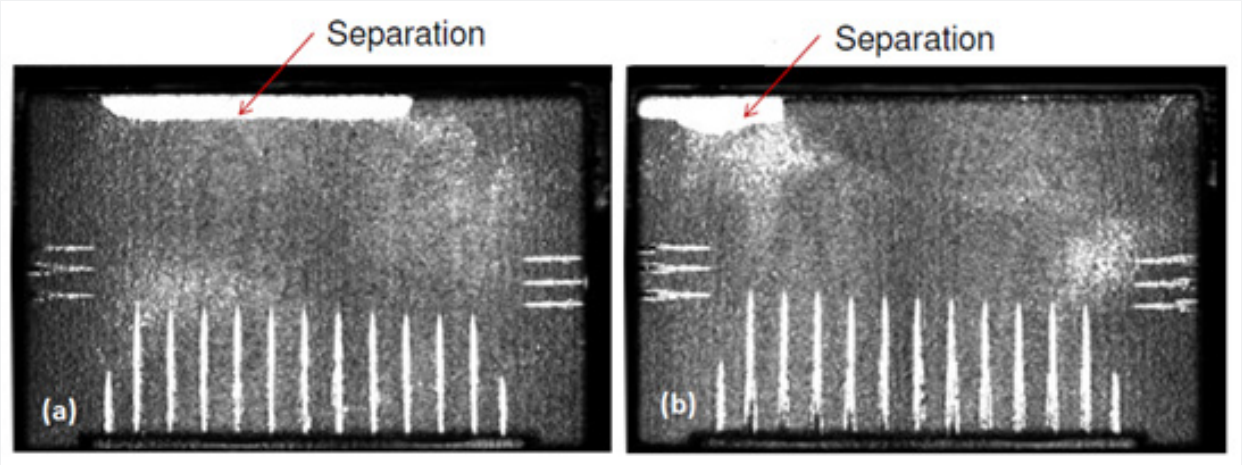

Figure 3: The debonding areas at the interface of the coating and the part are displayed in ultrasonic micro imaging inspection. (a) A separation area is indicated near the edge; (b) A separation area is indicated near the corner.

Ultrasonic inspection is a highly effective nondestructive testing method that is particularly well-suited for detecting the bonding condition between coatings and substrates. It has been extensively developed for various coating applications [18-20]. Compared to other methods, ultrasonic NDT inspection offers several advantages. It provides full volumetric information, delivers an immediate response, operates at a rapid speed, and only requires access to one surface. Additionally, it can determine flaw depth and location with high sensitivity and offers automation capabilities.

However, there are certain limitations to ultrasonic examination. These include the importance of flaw orientation, difficulty in interpreting results, challenges with complex geometries, the need for a liquid couplant, and the requirement for a smooth surface. In this specific case study, the part was tested after grinding to achieve a smooth coating surface. It was found that an as-sprayed part with a rough surface did not perform well in identifying interface defects. Furthermore, ultrasonic inspection is sensitive to material properties and uniformity due to the attenuation in acoustic velocity [21,22]. It is less effective in detecting vertically oriented defects such as coating cracking. The inspection results can be used to determine if the part conforms to the specified interface condition and whether it can be salvaged within the specified dimensions by removing the defective coating areas through grinding. Moreover, early discovery of non-conformed coating parts through ultrasonic inspection can lead to cost savings by avoiding subsequent process operations like fine finish grinding and post-heat treatment.

Interface inspection by pulsed thermograph

The thermograph technique offers several advantages over the ultrasonic technique, particularly when it comes to dealing with curved surfaces and surface roughness. Thanks to advancements in pulsed flashlight hardware and thermographic signal reconstruction (TSR) technology, high-resolution thermographic imaging can now be used to inspect parts with curved surfaces that are coated with a thick MCrAlY alloy coating using the HVOF deposition method. In Figure 5a, an area indicating potential coating separation can be seen during FBI inspection. An IR camera recorded a video of the pulsed response over time, and the 2D image captured at 0.12 seconds is displayed in Figure 5b. Certain isolated areas are highlighted, suggesting potential coating defects such as separation or large voids. One of these highlighted spots corresponds to the near-edge location of the coating separation previously detected in FPI (Figure 5a).

How to cite this article: Xinqing M, Peter R. Advances in Nondestructive Evaluation and Analyses of Thermal Spray Coatings. JOJ Material Sci. 2024; 8(4): 555744. DOI: 10.19080/JOJMS.2024.08.555744

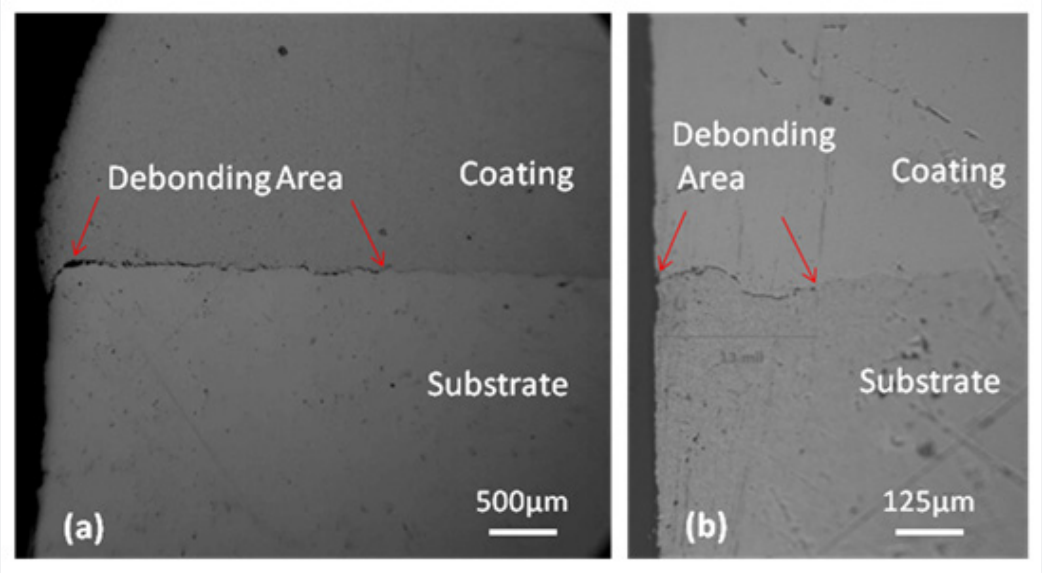

Figure 4: The coating separation shown in Figure 3b is confirmed by part cutup and metallographic examination. (a) Coating debonding in as-sprayed condition is exhibited before side surface grinding; (b) Coating debonding is exhibited in the same part after side surface grinding.

To further confirm the presence of coating debonding near the edge, 2D line profiles were drawn along the two edges (Figure 5c), and their profiles with location information were compared in Figure 5d. It is evident that the area at the central length of approximately 58 mm (2.28 inches) exhibits a strong reflected signal response from the left-side 2D line profile, in contrast to the right-side profile. Assuming the right-side line profile as a baseline without any "debonding" defect, the strong signal from the left-side profile indicates the detection of coating separation in that specific area. For comparison, another part coated with the same configuration and coating underwent FPI, which confirmed no coating separation. This part was further inspected using the same thermograph testing setup. The TSR 2D images shown in Figure 6 do not display any noticeable debonding area. The areas in the image that appear in white or black colors correspond to different depths from the heat input surface, rather than coating separation.

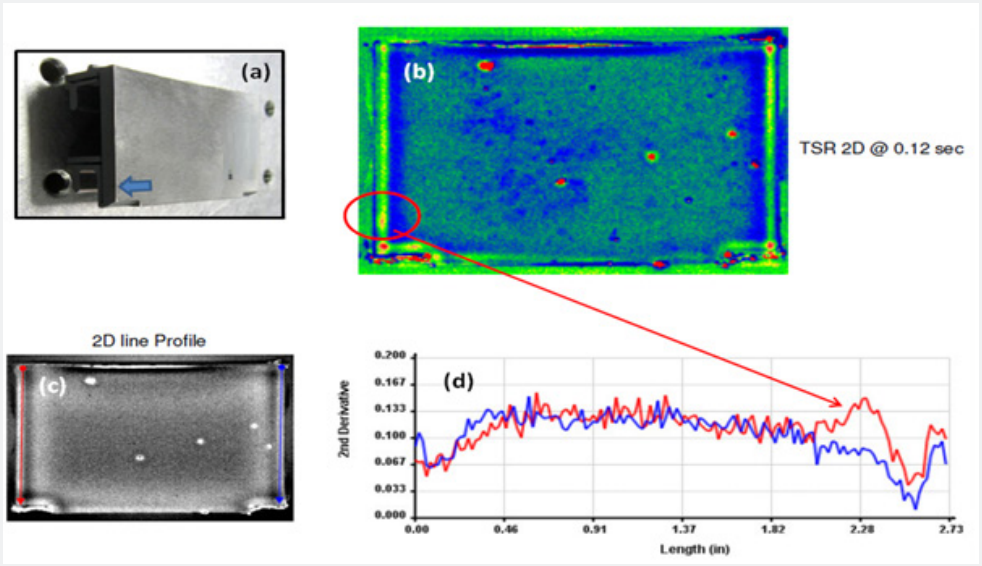

Figure 5: Thermographic imaging evaluation for the separation at the interface of thick HVOF alloy coating and part. (a) The coated part indicating a coating debonding in the arrowed area by FPI; (b) TSR 2D thermograph at the time of 0.12 second; (c) The 2D line profiles along the two edge areas (the left scan line in red and the right scan line in blue); (d) The profiles of the 2D line scanning.

How to cite this article: Xinqing M, Peter R. Advances in Nondestructive Evaluation and Analyses of Thermal Spray Coatings. JOJ Material Sci. 2024; 8(4): 555744. DOI: 10.19080/JOJMS.2024.08.555744

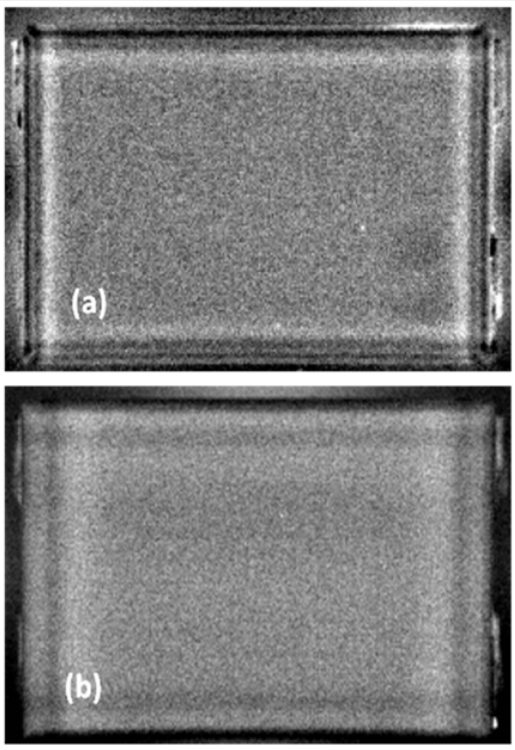

Figure 6: Thermographic imaging evaluation for the interfaces of thick HVOF alloy coating and part, indicating no coating separation. (a) TSR 2D thermograph at the time of 0.12 second; (b) TSR 2D thermograph at the time of 0.9 second.

The thermal pulsed imaging technique has demonstrated practicality and versatility in various demonstrations, making it suitable for a wide range of coatings [23-25]. Its advantages for infrared/thermal inspections include the ability to be conducted during operation, quantitative or qualitative analysis, easy-to-understand infrared images for customers, no requirement for a reference sample, suitability for curved surfaces, quick and safe measurements, and cost-effectiveness. However, drawbacks for infrared/thermal inspections may involve the impact of ambient conditions on accuracy, the need for heating/cooling in certain cases, distance-related errors, a requirement of DT > 3 °F, and unreliable readings from parts with double-wall or multiple hollow structures. The comparison of coating microstructure effects on thermal and ultrasonic wave propagation suggests that porous coatings have high ultrasonic wave attenuation and low thermal wave attenuation, explaining the success of thermal waves over ultrasonic waves in plasma sprayed coatings with high porosity [26].

The HVOF coating in this study exhibits minimal porosity (<1%), resulting in thermographic images with high resolution and detection depth of at least 2.5 mm through thick coatings. Moreover, the curved surface seems to have little impact on the TSR images. Therefore, the innovative thermographic method can address the current lack of widely available NDT testing methods for thermal spray coatings, as indicated in the thermal spray roadmap [27].

In-situ coating thickness measurement by Laser sensoring technique

It is crucial to conduct NDT inspections for coating defects, but there is also a pressing need for real-time, non-contact monitoring of coating thickness due to the lack of commercially available methods. Implementing a real-time thickness monitor can significantly reduce process time and costs, especially ensuring thickness compliance with specifications. Laser thickness sensing measurements involve recording initial dimensional data before coating deposition at specific locations, followed by in-situ dimensional data collection during the coating process. Figure 7 illustrates a standard data chart displaying dimensional measurements before and during the coating application in a spray cell. In Figure 7, the dimensional data were gathered repeatedly from a single location that was linked to a data I/O channel in the internal memory of the system. As the number of data samples increased over time, a thickness profile could be created and shown in real-time. The data point labeled as “F1” was taken from the surface of the part before the process, while the point “F2” was obtained from the coating surface during spray deposition. If the laser sensor remained fixed, only the thickness at one location was monitored. However, if the laser sensor was mounted on a programmed robot, thickness data from multiple locations could be collected.

How to cite this article: Xinqing M, Peter R. Advances in Nondestructive Evaluation and Analyses of Thermal Spray Coatings. JOJ Material Sci. 2024; 8(4): 555744. DOI: 10.19080/JOJMS.2024.08.555744

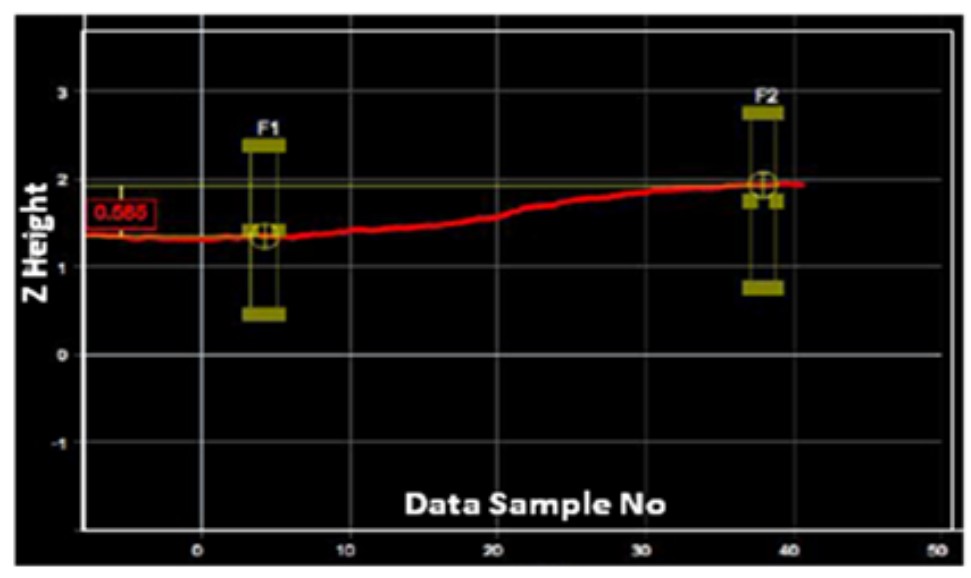

Figure 7: A data chart of laser thickness sensoring measurement during coating buildup in a thermal spray process.

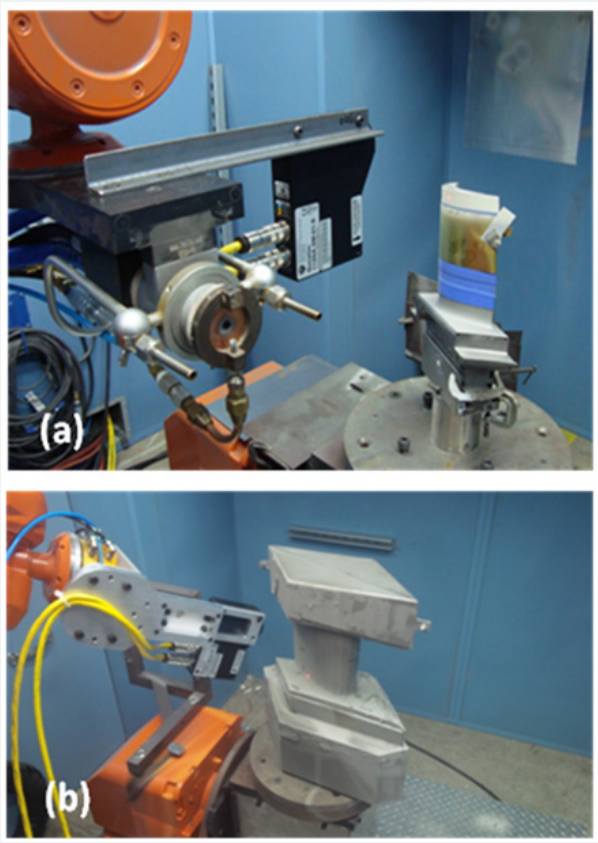

Figure 8: Photos of in-situ laser thickness measurement setups with the sensor mounted on a programmed robot. (a) Experimental setup for non-contact thickness monitor on a turbine blade with a thickness witness tab; (b) Experimental setup for non-contact thickness monitor on a turbine vane.

How to cite this article: Xinqing M, Peter R. Advances in Nondestructive Evaluation and Analyses of Thermal Spray Coatings. JOJ Material Sci. 2024; 8(4): 555744. DOI: 10.19080/JOJMS.2024.08.555744

Table 2: Experimental results for MCrAlY coating thickness measurement by in-situ laser sensor method and ex-situ methods. The measurements were performed on selected areas of airfoil, fillet and shroud on a turbine blade.

Measurement Locations	Average Coating Thickness Per Method, μm		
	Method-1	Method-2	Method-3
	Micrometer	Laser Sensor	Metallograph
Airfoil	178(0)	152 (-26)	178
Fillet	203(+12)	229 (+38)	191
Shroud	191(+13)	203(+25)	178

Figure 8 shows two experimental setups of laser thickness sensoring, one measurement on a turbine blade and another on a turbine vane. Due to the interference to the laser beam induced by the high brightness noise of thermal spray plume, the laser sensor was aligned with the thermal spray plume at 90 degrees and thickness measurement were measured at an interval of thermal spray cycles while the plume was moved away from the part. A position camera with pre-recorded features for the measurement locations could be used to automatically identify the sampling locations and trigger the data recordings repeatedly. Achieving full automation and precise measurement is possible when applying a layer to a complex configuration component. Additionally, the control system can establish a threshold value for the minimum or maximum thickness. By utilizing the system I/O output from the laser sensor and input to the thermal spray control console, a closed-loop control system can be created to halt the process once the dimensional data shows that the minimum or maximum thickness has been attained.

The investigation involved assessing the accuracy of thickness measurement by comparing results obtained through various methods. In Table 2, the thickness results from three different methods are presented and compared for measurements taken at specific locations on a turbine vane, as illustrated in Figure 8b. When comparing the results to the metallographic examination conducted using optical microscopy as a reference point, it was observed that the pin-micrometer measurements on the witness tabs consistently yielded higher values. The laser measurements at three locations showed variations ranging from -26 μm to +38 µm compared to the baseline values. Considering a typical coating thickness tolerance of -/+50 μm, the results obtained from the laser sensor method fall within an acceptable range.

Essential for a coating process, especially when applied to turbine components. Currently, coating thickness is often confirmed through indirect methods on witness tabs using a micrometer or through ex-situ metallographic examination after destructively sectioning the coated part. Non-conformance to specified coating thickness levels frequently leads to a high rework rate, particularly in the thermal spray industry. Advanced technologies have been developed to address quality concerns related to coating thickness control and uniformity, serving as inspection tools for checking coating thickness on industrial components. Laser or blue-light 3D scanning techniques can determine coating thickness across the entire surface of a coated part by analyzing 3D scanning data before and after the coating process in an inspection area. Based on the thickness data presented in Table 2, the real-time accuracy of the Laser thickness sensing method can be compared to the results obtained from ex-situ destructive tests. In relatively flat regions, such as the shroud, the thickness values are similar. However, in curved areas like the airfoil and fillet, there are noticeable variations in the mean values. Additionally, considering the Std values, it appears that the laser in-situ measurement method has a wider error range compared to the two ex-situ measurement methods.

However, it is important to note that these methods are primarily used for ex-situ thickness inspection, rather than as in-situ thickness monitoring or control tools. Therefore, the in-situ laser sensoring method for real-time coating thickness monitoring and control is a unique, beneficial, and valuable tool for thermal spray operations. The accuracy of in-situ and ex-situ measurement methods can be explained by considering the factors that affect the accuracy of in-situ laser measurement. These factors include the impact of surface roughness on laser reflection, as light scattering is influenced by the roughness of the surface. Consequently, the measurement can yield more errors when the surface is rougher. Additionally, the repeatability or correlation of measurement spots or positions can vary due to mismatched locations before and after coating, resulting in significant measurement errors. Moreover, the accuracy and repeatability of laser position may be limited by the accuracy or resolution of the vision camera used to identify the unique features, colors, or marks on the surface to determine the measurement spots. Furthermore, the fixture used to hold the test pieces may become loose and move during the measurement, altering the part orientation in three dimensions and consequently affecting the measurement results. Ideally, laser measurement is conducted on a two-dimensional surface, which explains the large deviations in measurement data observed in curved airfoil and fillet areas.

Despite its advantages, the laser thickness sensoring method has some limitations, such as restricted access to certain coating areas due to limited laser reference distance, inability to measure simultaneously while the thermal spray torch is targeting the coating area, measurement accuracy depending on consistent

How to cite this article: Xinqing M, Peter R. Advances in Nondestructive Evaluation and Analyses of Thermal Spray Coatings. JOJ Material Sci. 2024; 8(4): 555744. DOI: 10.19080/JOJMS.2024.08.555744

laser beam targeting, and a limited number of measurement locations due to system I/O channel availability. In the current study, a line-type or spot-type sensor with an extended reference distance was selected for thickness measurement, offering the advantage of reduced sensitivity to surface finish conditions.

Conclusion

Nondestructive evaluation, inspection, and testing (NDE, I&T) techniques play crucial roles in characterizing properties, developing processes, and ensuring quality control of various thermal spray coatings. The continuous need for advanced NDE techniques with non-contact and in-situ capabilities to measure coating characteristics quickly and accurately is evident. This study explores the latest NDE techniques through various case studies of thermal sprayed coatings, leading to the following key findings:

a) Laser confocal microscopy effectively characterizes surface morphologies and roughness profiles of HVOF coatings in a non-contact manner. The use of 2D profiles and 3D mapping allows for a comprehensive description of surface finish parameters across the entire coating surface.

b) Ultrasonic micro imaging proves successful in detecting interface separation, providing information on qualitative defective types and quantitative defective locations and areas. Comparative studies with destructive checks show a strong correlation in determining coating separation.

c) Thermographic pulse-echo imaging enables rapid detection of coating defects in turbine parts. The time-dependent thermal wave imaging delves into the coating matrix at different depths, offering a clear indication of interface defects.

d) Laser thickness sensing method is established for in-situ coating thickness measurement during real-time processing in a spray cell. This method delivers comparable accuracy in coating thickness measurement when compared with results from ex-situ destructive tests.

Acknowledgment

The authors wish to express their gratitude for the technical assistance and experimental support provided by Mr. David Reynolds and Mr. Samuel Greenbank from the Engineering Department at Curtiss-Wright Surface Technologies in East Windsor, CT.

References

1. Crostack HA (2001) NDT of Coatings, Surface Modified Layers, and Adhesives. In: Encyclopedia of Materials: Science and Technology (2nd Edn.), Elsevier Science Ltd. pp. 5977-5979.
2. Balageas D, Maldague X, Burleigh D, Vavilov VP, Oswald TB, et al. (2016) Thermal (IR) and other NDT techniques for improved material inspection. J Nondestruct Eval 35(18): 1-17.
3. Almond D, Patel P (1985) Thermal-wave testing of plasma-sprayed coatings and a comparison of the effects of coating microstructure on the propagation of thermal and ultrasonic waves. J Mater Sci 20: 955-966.
4. Hanlon DN, Todd I, Peekstok E, Rainforth WM, Zwaag S (2001) The Application of laser scanning confocal microscopy to tribological research. Wear 251(1-12): 1159-1168.
5. Hovis DB, Heuer AH (2010) The use of laser scanning confocal microscopy (LSCM) in materials science. J Microscopy 240(3): 173-180.
6. Hsueh CH, Haynes JA, Lance MJ, Becher PF, Ferber MK, et al. (1999) Effects of interface roughness on residual stresses in thermal barrier coatings. J Am Ceram Soc 82(4): 1073-1075.
7. Hovis D, Hu L, Reddy A, Heuer AH, Paulikas AP, et al. (2007) *In situ* studies of the TGO growth stresses and the martensitic transformation in the B2 phase in commercial Pt-modified NiAl and NiCoCrAlY bond coat alloys. Int J Mater Res 98: 1209-1213.
8. Merson E, Danilov V, Merson D, Vinogradov A (2017) Confocal laser scanning microscopy: The technique for quantitative fractographic analysis. Engineering Fracture Mechanics 183: 147-158.
9. Maldague XP (2001) Theory and Practice of Infrared Technology for Nondestructive Testing. A Wiley-Interscience Publication (New York).
10. Ptaszek G, Cawley P, Almond D, Pickering S (2012) Artificial disbonds for calibration of transient thermography inspection of thermal barrier coating systems. NDT&E International 45(1): 71-78.
11. Newaz G, Chen X (2003) Progressive damage assessment in thermal barrier coatings using thermal wave imaging technique. Surf. Coatings and Technol 190: 7-14.
12. Vavilov VP, Burleigh D (2015) Review of pulsed thermal NDT: Physical principles, theory and data processing. NDT&E International 73: 28-52.
13. Oehler H, Alig I, Lellinger D, Bargmann M (2012) Failure modes in organic coatings studied by scanning acoustic microscopy. Progress in Organic Coatings 74(4): 719-725.
14. Kwak DR, Yoshida S, Sasaki T, Todd JA, Park IK (2016) Evaluation of near-surface stress distributions in dissimilar welded joint by scanning acoustic microscopy. Ultrasonics 67: 9-17.
15. Maev R (2016) Acoustic Microscopy for Materials Characterization, in Materials Characterization Using Nondestructive Evaluation (NDE) Methods. In: Hubschen G, Altpeter I, Tschuncky R, Herrmann HG, WP/ Woodhead Publishing, New York, USA, pp. 161-175.
16. Ma X, Ruggiero P (2013) Ultrasmooth, dense hardface coating applied by advanced HVOF process. Advanced Materials and Processes 171(2): 36-38.
17. Ma X, Ruggiero P (2014) Ultra-smooth hardface coatings applied by advanced HVOF process. Proc Int'l Symp for Thermal Spray Conference and Exposition, Barcelona, Spain, May, pp. 285-290.
18. Chen H, Zhang B, Alvin M, Lin Y (2012) Ultrasonic detection of delamination and material characterization of thermal barrier coatings. J Thermal Spray Technol 21(6): 1184-1194.
19. Lescribaa A, Vincent A (1996) Ultrasonic characterization of plasma sprayed coatings. Surface and Coating Technology 81(2-3): 297-306.
20. Fabbri L, Oksanen M (1999) Characterization of plasma-sprayed coatings using nondestructive evaluation techniques: Round-Robin test results. J Thermal Spray Technol 8(2): 263-272.
21. Ma X, Mizutani Y, Takemoto M (2001) Laser-induced surface acoustic waves for evaluation of elastic stiffness of plasma sprayed materials. J Mater Sci 36: 5633-5641.

How to cite this article: Xinqing M, Peter R. Advances in Nondestructive Evaluation and Analyses of Thermal Spray Coatings. JOJ Material Sci. 2024; 8(4): 555744. DOI: 10.19080/JOJMS.2024.08.555744

22. Fei D, Hsu D, Warchol M (2001) Simultaneous velocity, thickness and profile imaging by ultrasonic scan. J Nondestructive Evaluation 20(3): 95-112.

23. Green D, Wandung C, Gatto F, Rogers FS (1985) System for NDE of thermal spray coating bonds. J Materials for Energy Systems 7(3): 276-284.

24. Sargent J, Almond D, Gathercole N (2006) Thermal wave measurement of wet paint film thickness. J Mater Sci 41: 333-339.

25. Spicer M, Kerns J, Aamodt W, Murphy JC (1989) Measurement of coating physical properties and detection of coating disbonds by time resolved infrared radiometry. J Nondestruct Eval 8(2): 107-120.

26. Patel PM, Almond DP (1985) Thermal wave testing of plasma-sprayed coatings and a comparison of the effects of coating microstructure on the propagation of thermal and ultrasonic waves. J Mater Sci 20(3): 955-966.

27. Vardelle A, Moreau C, Akedo J, Ashrafizadeh H, Berndt CC, et al. (2016) The 2016 thermal spray roadmap. J Thermal Spray Technol 25(8): 1376-1440.

28. Sharma A, Dudykevych T, Sansom D, Subramanian R (2017) Increased reliability of gas turbine components by robust coatings manufacturing. J Thermal Spray Technol 26: 1084-1094.

29. Song X, Meng F, Kong M, Wang Y, Huang L, et al. (2016) Thickness and microstructure characterization of TGO in thermal barrier coatings by 3D reconstruction. Materials Characterization 120: 244-248.

30. Bienias M, Gao S, Hasche K, Seemann R, Thiele K (1998) A metrological scanning force microscope used for coating thickness and other topographical measurements. Applied Physics A 66: 837-842.

DOI: 10.19080/JOJMS.2024.08.555744

How to cite this article: Xinqing M, Peter R. Advances in Nondestructive Evaluation and Analyses of Thermal Spray Coatings. JOJ Material Sci. 2024; 8(4): 555744. DOI: 10.19080/JOJMS.2024.08.555744